HETEROCYCLES, Vol. 96, No. 12, 2018, pp. 2096 - 2105. © 2018 The Japan Institute of Heterocyclic Chemistry
Received, 15th November, 2018, Accepted, 4th December, 2018, Published online, 7th December, 2018
DOI: 10.3987/COM-18-14014

BREVISULCENAL-G, -H, and –I, POLYCYCLIC ETHER MARINE TOXINS FROM THE DINOFLAGELLATE *KARENIA BREVISULCATA*

Masayuki Satake,[1]* Raku Irie,[1] Yuka Hamamoto,[1] Kazuo Tachibana,[1] Patrick T. Holland,[2] D. Tim Harwood,[2] Feng Shi,[2] Veronica Beuzenberg,[2] Yoshiyuki Itoh,[3] Fumiaki Hayashi,[4] and Huiping Zhang[4]

[1]Department of Chemistry, School of Science, The University of Tokyo, Hongo, Bunkyo-ku, Tokyo 113-0033, Japan. [2]Cawthron Institute, Private Bag 2, Nelson 7010, New Zealand. [3]MS Business Unit, JEOL Ltd., 3-1-2 Musashino, Akishima, Tokyo 196-8558, Japan. [4]Advanced NMR Application and Platform Team NMR Research and Collaboration Group NMR Science and Development Division RIKEN Spring-8 Center, 1-7-22, Suehiro-cho, Tsurumi-ku, Yokohama 230-0045, Japan. E-mail: msatake@chem.s.u-tokyo.ac.jp

Abstract – Members of two classes of marine polycyclic ether compounds, brevisulcenals (KBTs) and brevisulcatic acids (BSXs), were isolated as causative toxins from a red tide (*Karenia brevisulcata*) bloom event in New Zealand in 1998. The new analogues, brevisulcenals (KBTs)-G, -H, and -I, were isolated from neutral lipophilic extracts of bulk dinoflagellate culture extracts, and the molecular structures of these compounds were elucidated by detailed analyses of NMR and matrix-assisted laser desorption/ionization tandem mass spectrometry spectra, and by comparison with the spectra of KBT-F. All the analogues have the same size and arrangement of 24 ether rings, but differ in their backbone substitution patterns and degree of terminal oxidation. The cytotoxicity of these new KBT analogues was greater than that of the co-isolated, KBT-F.

INTRODUCTION

A new dinoflagellate species *Karenia brevisulcata*[1] formed a widespread bloom in the central and southern east coast of the North Island of New Zealand in early 1998, and resulted in massive kills of fish and other marine organisms in Wellington Harbour.[2] The bloom also caused over 500 cases of human respiratory distress with symptoms including a dry cough, severe sore throat, runny nose, skin and eye irritations, severe headaches and facial sun-burn sensations.

Cell extracts of *K. brevisulcata* exhibited strong mouse lethality and cytotoxicity, and during initial investigations were partitioned between chloroform and aqueous methanol (MeOH) under neutral conditions. Two different kinds of toxins were detected.[3] The aqueous MeOH layer contained brevisulcatic acids (BSXs), compounds that had brevetoxin-like ladder-frame polyether backbones and side-chain carboxylic acids, and which demonstrated toxicity against neuro2A cells.[4,5] The lipophilic layer contained brevisulcenals (initially named karenia brevisulcata toxins (KBTs) in ref. 3) and these showed strong mouse lethality and cytotoxicity against the P388 (murine leukemia) cell line.

NMR and matrix-assisted laser desorption/ionization (MALDI) tandem mass spectrometry (MS) with high-energy collision-induced dissociation (HE-CID) analyses led to the elucidation of the structure of one of the most abundant KBTs, and this compound was designated brevisulcenal-F (KBT-F, **1**).[6] KBT-F has the molecular formula $C_{107}H_{160}O_{38}$, and is a giant planar polycyclic ether compound comprising 24 ether rings, including a dihydrofuran, decorated with 13 hydroxy groups, 13 methyl groups (seen as two doublets and 11 singlets in the ^{1}H NMR spectrum), and a 2-methylbut-2-enal side-chain. KBT-F contains 17 contiguous ether rings A-Q, which are the longest of known polycyclic ethers. The long contiguous ether ring assembly with the 2-methylbut-2-enal terminus is similar to those of gymnocins A and B isolated from *Karenia mikimotoi*.[7] Even though KBT-F and the gymnocins had the same side chain structure, KBT-F showed potent mouse lethality and cytotoxicity against P388 cells at 50 ng/mL, while the gymnocins showed moderate cytotoxicity (1700 ng/mL). The structural elucidation of KBT analogues is important for determining the mode of action of these toxins, which may assist developing strategies to prevent the effects of KBT red tide events, should they occur again. Our ongoing efforts in this area have led to the isolation of three new KBT analogues, brevisulcenals-G (KBT-G, **2**), -H (KBT-H, **3**), and -I (KBT-I, **4**). In this paper we report the structural elucidation of **2**, **3**, and **4** by spectroscopic methods.

RESULTS AND DISCUSSION

Brevisulcenals (KBTs) were extracted from mature bulk cultures of *Karenia brevisulcata* using a resin-based isolation. Cells were lysed with acetone and after stirring for one hour, the cultures were diluted with water and passed through HP20 resin. Brevisulcenals were recovered by washing the resin with acetone, dissolving the lyophilized extract in 55% MeOH and pH 7.2 phosphate buffer, and then extracting the lipophilic toxins with chloroform. The chloroform extract was chromatographed on a diol-silica column with stepwise elution of ethyl acetate (EtOAc), EtOAc:MeOH (9:1, 8:2, 7:3, 6:4), MeOH and guided by cytotoxicity assay against mouse leukemia P388 cells. Further purification of KBTs was performed using reversed phase chromatography with 90% MeOH/H_2O. Final purification of KBTs was achieved through reversed phase chromatography with 85% MeOH/H_2O with monitoring by UV absorbance at 230 nm. This isocratic elution enabled chromatographic separation of the very closely

eluting KBT-F (**1**) and KBT-G (**2**). Similarly, repeated reverse phase steps with 90% MeOH/H_2O followed by 85% MeOH/H_2O were required to chromatographically resolve KBT-H (**3**) and KBT-I (**4**). These separations yielded **1** (3.1 mg), **2** (1.3 mg), **3** (1.2 mg), and **4** (0.6 mg). In an analogous fashion, ^{13}C-enriched KBTs **1** (1.9 mg), **2** (0.6 mg), **3** (0.9 mg), and **4** (0.4 mg) were obtained from cultures grown in media containing ^{13}C-$NaHCO_3$.

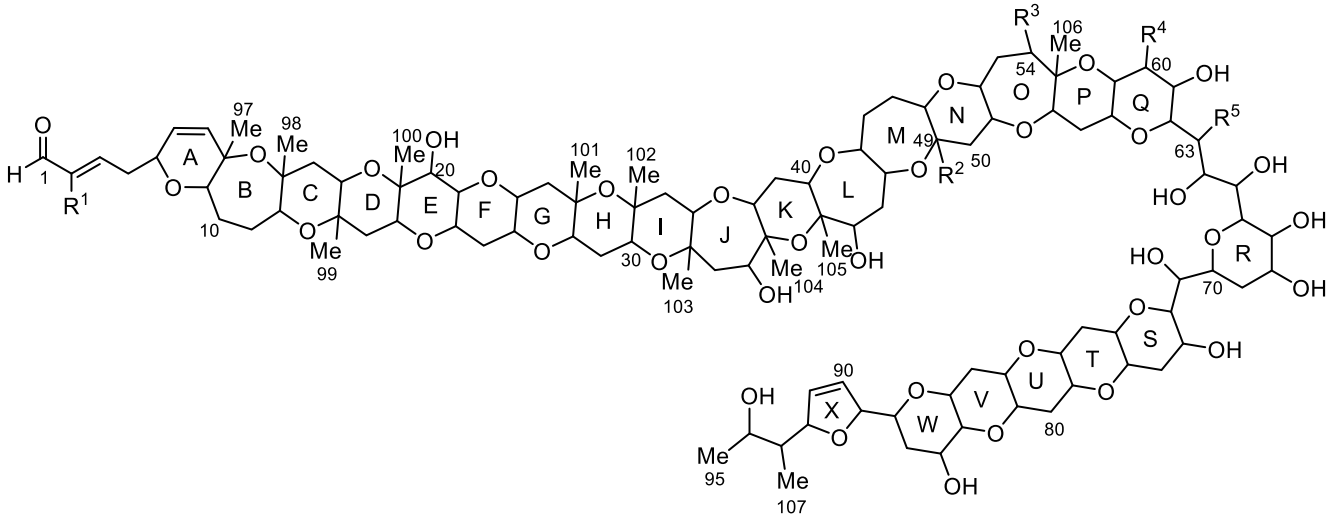

	R^1	R^2	R^3	R^4	R^5
KBT-F (**1**)	Me	H	H	OH	H
KBT-G (**2**)	Me	Me (108)	OH	H	OH
KBT-H (**3**)	CH_2OH	H	H	OH	H
KBT-I (**4**)	CH_2OH	Me (108)	OH	H	OH

Figure 1. Structures of KBT-F (**1**), KBT-G (**2**), KBT-H (**3**), and KBT-I (**4**)

A UV absorption maximum at 228 nm indicated that **2** possessed a 2-methylbut-2-enal side-chain, identical to that in **1**. A sodium adduct ion peak of **2** was observed in the positive ion MALDI mass spectrum at *m/z* 2106, and was 30 u larger than that of **1**. The accurate mass measurement by the MALDI-SpiralTOF[8] and ^{1}H and ^{13}C NMR spectra (collected primarily on 800 and 500 MHz instruments) indicated that the molecular formula of **2** was $C_{108}H_{162}O_{39}$ ($[M+Na]^+$ 2106.0584, calcd. 2106.0585), suggesting that the 30 u difference between **1** and **2** corresponded to CH_2O. Comparison of the ^{13}C NMR spectra of **1** and **2** did show that an extra methyl group, and an extra hydroxy group, were present in **2**.

In the ^{13}C NMR and HSQC spectra of **2**, 12 methyl singlets and 11 oxygenated quaternary carbons were observed. This indicated **2** had 11 angular methyls between its ether rings, and one olefinic methyl. In comparison, there were ten angular methyl groups in **1**, meaning one angular proton in **1** (H-49) was substituted with a methyl in **2**. Moreover, it suggested that the carbon chain of **2** was 95 atoms long, which was identical to that of **1**, and meant that the ether ring backbone of **2** was similar to that of **1**. The

observation of 24 methylenes and a methine carbon in an aliphatic region, and 51 oxygenated methine carbons, confirmed that an aliphatic methylene in **2** was connected to an oxygenated methine carbon. The COSY and HSQC spectra also suggested that the number of hydroxy groups in **2** was different to that in **1**. Detailed analysis of ^{1}H-^{1}H COSY and TOCSY spectra led to identification of spin systems. The partial structures H-3 to H-7, H-9 to H-12, H-14 to H-15, H-17 to H-18, H-20 to H-26, H-28 to H-30, H-32 to H-33, H-35 to H-36, H-38 to H-40, H-42 to H-48 and H-66 to Me95 in **2** were identical to those of **1**. The ^{13}C chemical shift at δ_C 11.4 for Me96 and the NOE correlation Me96/H-4a indicated an *E* configuration of Δ^2. This suggested that structural differences between **1** and **2** resided on a portion from C49 to C65. An HSQC signal for an oxygen-bearing methine carbon, which corresponded to CH49 in **1**, was not observed. Therefore, the new methyl singlet was deduced to be positioned on C49. This was supported by analysis of the HMBC spectrum for **2**, which revealed correlations from a methyl singlet to C48, C49 and C50. Thus the position of the substituted methyl (Me108) was confirmed as being C49. The presence of a hydroxy group on C54 was also determined by a proton correlation between the methylene at H-53 and the oxygenated methine at H-54 and the HMBC correlation from Me106 to the oxygenated methines (C54 and C56). Structural differences in **2** from H-60 to H-63, compared to the same section of **1**, were also deduced by detailed analyses of COSY and HSQC spectra. A COSY correlation revealed the proton connectivity from H_2-60 to H-63. Proton couplings between H-63/H-64 and H-65/H-66 were not observed in the COSY of **2**, and this was probably due to suboptimal dihedral angles and lack of sample. NOE correlations H-63/H-64 and H-65/H-66 enabled connectivity to be assigned from H-63 to H-66. It was apparent at this stage that **2** differed from **1** in having a methyl between rings M and N, hydroxy groups on C54 and C63, and no hydroxy substitution on C60. The ^{1}H NMR chemical shifts of rings S-W of **2** were also different to those in the analogous region of **1**, which suggested that structural differences in rings M-R of **2** must alter the chemical environment of protons of rings S-W.

Table 1. NMR spectroscopic data (800 MHz, pyridine-d_5) for brevisulcenal-G (**2**)

Pos.	δ_H (*J* in Hz)	δ_C	Pos.	δ_H (*J* in Hz)	δ_C	Pos.	δ_H (*J* in Hz)	δ_C
1	9.54, s	197.1	36	4.12, m	78.3	71	5.05, m	67.1
2		143.3	37		82.7	72	4.21, m	82.6
3	6.61, dd (5,5)	151.9	38	4.35, m	80.0	73	4.57, m	66.8
4a	2.46, m	36.6	39a	2.14, m	32.8	74a	2.44, m	41.6
4b	2.56, m		39b	2.35, m		74b	2.83, m	
5	4.37, m	76.2	40	4.18, m	78.0	75	3.36, m	79.7
6	5.45, d (10)	127.0	41		82.7	76	3.66, m	78.6
7	5.98, dd (2, 10)	139.9	42	4.05, m	75.6	77a	1.79, m	38.1
8		78.3	43a	2.25, m	42.8	77b	2.63, m	
9	3.85, d (10)	80.0	43b	2.50, m		78	3.42, m	79.5
10a	1.97, m	26.4	44	4.18, m	73.3	79	3.41, m	80.0
10b	2.04, m		45	4.18, m	85.6	80a	2.20, m	37.8
11a	1.90, m	26.7	46a	2.16, m	35.2	80b	2.61, m	

11b	2.05, m		46b	2.48, m		81	3.36, m	79.7
12	4.07, m	75.4	47a	1.76, m	27.2	82	3.42, m	79.5
13		81.4	47b	2.06, m		83a	1.74, m	38.4
14a	2.05, m	43.7	48	3.27, m	88.5	83b	2.46, m	
14b	2.08, m		49		78.3	84	4.28, m	66.6
15	3.90, d (10)	72.7	50a	1.91, m	49.3	85	3.27, m	83.3
16		76.4	50b	2.48, m		86	4.40, m	67.4
17a	2.00, m	41.6	51	4.37, m	79.7	87a	2.02, m	34.0
17b	2.24, m		52	3.52, m	83.0	87b	2.61, m	
18	4.53, m	74.2	53a	2.10, m	39.0	88	3.75, m	78.6
19		79.6	53b	2.30, m		89	5.98, brs	87.1
20	4.39, m	75.1	54	4.06, m	76.8	90	6.17, d (5)	132.0
21	3.67, m	82.4	55		82.0	91	6.41, d (5)	132.3
22	4.20, m	75.4	56	4.29, m	77.1	92	5.21, m	90.9
23a	1.90, m	38.1	57a	2.16, m	34.9	93	1.62, m	48.7
23b	2.73, m		57b	2.33, m		94	4.44, m	68.0
24	3.43, m	81.8	58	3.25, m	80.9	95	1.37, d (7)	23.1
25	3.59, m	80.6	59	3.76, m	71.2	96	1.74, s	11.4
26a	1.76, m	46.3	60a	1.75, m	41.9	97	1.47, s	24.3
26b	2.39, m		60b	2.52, m		98	1.59, s	23.4
27		76.3	61	4.66, m	73.0	99	1.48, s	17.3
28	3.46, m	85.9	62	4.14, m	82.4	100	1.50, s	17.6
29a	2.02, m	30.2	63	4.99, m	76.8	101	1.47, s	24.3
29b	2.07, m		64	5.26, m	72.7	102	1.69, s	23.4
30	3.67, m	76.2	65	4.97, m	73.6	103	1.58, s	22.8
31		77.2	66	4.44, m	76.5	104	1.40, s	21.4
32a	1.91, m	44.8	67	4.50, m	75.4	105	1.40, s	23.7
32b	2.41, m		68	4.50, m	72.1	106	1.41, s	17.0
33	4.89, m	80.9	69a	2.19, m	35.5	107	1.09, d (6)	11.7
34		81.7	69b	3.16, m		108	1.46, s	18.2
35a	2.31, m	48.4	70	4.73, m	74.2			
35b	2.60, m							

Since MALDI tandem MS with HE-CID using a MALDI-SpiralTOF-TOF[9] instrument was determined to be useful for the structural determination of **1**,[6] structural confirmation of **2** was also conducted with the same experimental setup (Figure 2). Given that **2** does not have a suitable terminal charge site for a negative ion tandem MS measurement, it was reacted with 3-(hydrazinecarbonyl)benzene sulfonate in 80% pyridine.[6] The resulting benzene sulfonate adduct gave an ion at *m/z* 2280, and this was selected as a precursor ion for the HE-CID tandem MS experiments. A product ion was observed at *m/z* 1193 for both **1** and **2**. In addition, the product ions observed below *m/z* 1193 of **2** were identical to that of **1**, confirming that the partial structure of **2** from the terminal aldehyde to ring L (C1 to C46) had the same molecular composition to that in **1**. The different product ions observed in the range of *m/z* 1100-1700 for **1** and **2**, suggested that the structural differences between **1** and **2** existed on rings M to R (C49-C64). As shown in Figure 2, prominent product ions at *m/z* 1193, 1277, 1333, 1433, and 1489 were observed in the spectrum of **2**, and the mass differences between those product ions were 84, 56, 100, and 56 u respectively. The presence of these ions strongly supported that rings M to P comprised a 7-membered ether ring with a

methyl, a 6-membered ether ring, a 7-membered ether ring with a methyl and a hydroxy, and a 6-membered ether ring, respectively. The mass difference of 56 u between product ions at *m/z* 1545 and *m/z* 1489 confirmed that the hydroxy group at C60 on ring Q was not substituted in **2**. These data explained the structures of the rings M, N, O, Q, and in addition the product ion at *m/z* 1621 showed a hydroxy group resided on C63. The product ions of **2**, which were greater than *m/z* 1621 gave signals that were 30 u greater than those of **1** which corresponded to an extra CH_2O being present in **2** (as mentioned above). Thus, the planar structure of **2** was elucidated as shown Figure 1. Elucidation of the stereostructure of **2** is now under way by synthetic methods.[10]

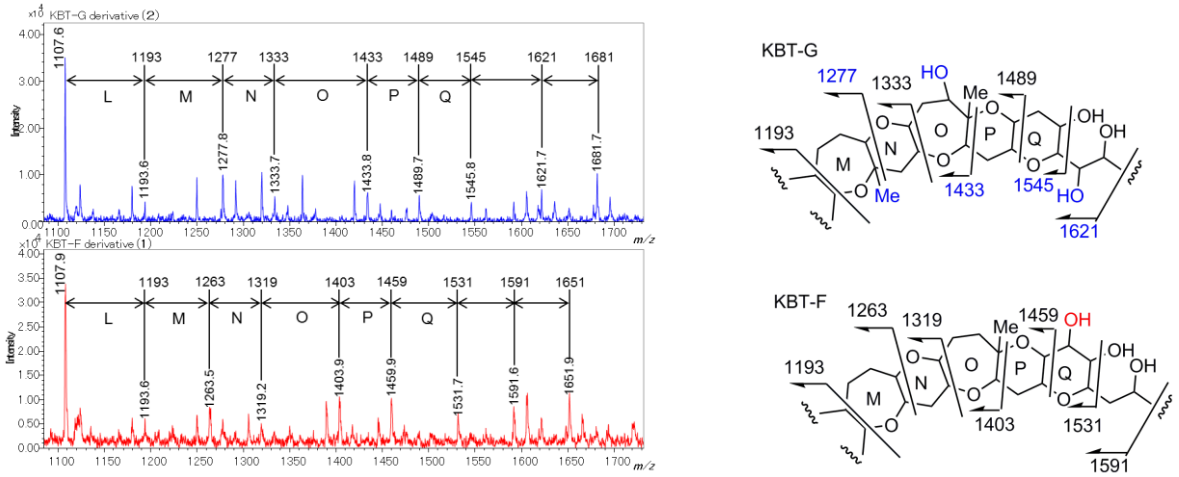

Figure 2. Comparison of important product ions of rings M-Q in **2** (top) and **1** (bottom) by TOF-TOF experiments and assignment of cleavage sites in **1** and **2**

The molecular formula of **3** was determined as $C_{107}H_{160}O_{39}$ ($[M + Na]^+$ 2092.0422, calcd 2092.0429 for $C_{107}H_{160}O_{39}Na$) by the accurate mass measurement with a MALDI-SpiralTOF. This is 16 u larger than that of **1**, which has a molecular formula of $C_{107}H_{160}O_{38}$. Thus, it appeared that the presence of one additional oxygen was present in **3**. The observed aldehyde signal in the ^1H NMR spectra eliminated the possibility that this was due to oxidation of an aldehyde to a carboxylic acid. However, the downfield shift of the aldehyde peak of **3** (δ_H 9.64) relative to the analogous peak of **1** (δ_H 9.51), combined with the absence of an olefinic methyl peak for **3** (δ_H 1.73 in **1**) suggested that the 2-methylbut-2-enal terminus of **3** was structurally different to **1**. In the HSQC spectrum of **3**, most of the observed signals were similar to those of **1**, and an unambiguous difference was that a C96 olefinic methyl signal was not observed in the HSQC spectrum of **3**, but that an oxymethylene signal was detected at δ_H 4.67 and δ_C 56.2 (Figure 3). This suggested that the olefinic methyl at the enal terminus of **1** was oxidized to a hydroxymethylene in **3**. The position of this hydroxymethylene was confirmed by the HMBC correlations from the hydroxymethylene proton (H_2-96) to C1 (δ_C 196.6), C2 (δ_C 147.4), and C3 (δ_C 152.0). The remaining

HSQC signals of **3** were identical to those of **1**. Therefore, the structure of **3** was elucidated as that shown in Figure 1. This branched hydroxymethylene moiety of **3** is previously unknown in dinoflagellate-derived metabolites. In brevetoxins[11] and gymnocins,[7] the terminal aldehydes are instead oxidized to carboxylic acids.

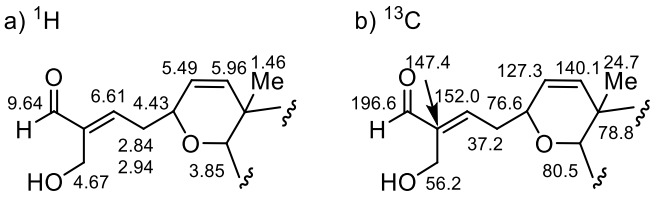

Figure 3. Partial ^{1}H (a) and ^{13}C (b) chemical shift assignments (δ) of **3** and **4** in pyridine-d_5

The molecular formula of **4** was determined to be $C_{108}H_{162}O_{40}$ ($[M + Na]^+$ 2122.0532, calcd 2122.0535 for $C_{108}H_{162}O_{40}Na$) by MALDI-SpiralTOF and showed **4** was 16 u larger than that of **2**. This suggested that **4** was an allylic primary alcohol analogue of **2**, and the confirmatory oxymethylene signal was detected at δ_H 4.67 and δ_C 56.2 in the HSQC of **4**. The HMBC correlations from the hydroxymethylene (H_2-96) to C1, C2, and C3 confirmed that **4** had a 2-hydroxybut-2-enal side chain analogous to **3**. Therefore the planar structure of **4** was elucidated as shown in Figure 1.

Details of the observed biological properties of KBTs have been reported previously.[3] Mouse lethality of **2** was estimated to be 0.032 mg/kg. Cytotoxicity of **1**, **2**, **3**, and **4** against mouse leukemia P388 cells were determined to be 2.7, 0.7, 1.6, and 0.14 nM, respectively. This shows that the oxidized olefinic (hydroxymethylene) terminus of **3** and **4** slightly enhanced their cytotoxicity relative to that of **1** and **2**. The structures of three new brevisulcenal (KBT) analogues were elucidated by NMR and tandem MS experiments. All the analogues have the same size and arrangement of 24 ether rings, but differ in their backbone substitution patterns and degree of terminal oxidation. The branched primary alcohols of **3** and **4** were deduced to be generated by oxidation of olefinic methyls in the side chains of **1** and **2**, respectively. Such oxidation of branched methyls is very rare among secondary metabolites from dinoflagellates. The greater cytotoxicity of **3** and **4** than that of **1** and **2** indicates that this oxidation of the olefinic methyls enhances their toxicity. The structures of KBTs are reminiscent of the structure of maitotoxin,[12] the largest non-biopolymer natural product, in that they possess rigid polyether assembles linked by flexible linear alkyl chains and the molecules have hydrophobic (rings A-Q) and hydrophilic (the linker part and rings R-X) portions. The mode of actions of KBTs has not yet been determined, although it is plausible that the strong toxicity of these molecules results from their interaction with membrane proteins, akin to the mode of action of other marine ladder-frame polyether toxins.

EXPERIMENTAL

General methods. All solvents were purchased at highest commercial grade and used as supplied unless otherwise noted. Optical rotations were obtained on a JASCO DIP-350 polarimeter in MeOH. UV-visible absorption spectra were measured on a JASCO V-550 UV-spectrometer. NMR spectra were recorded on three NMR instruments: 500 MHz (125 MHz for ^{13}C), 400 MHz (100 MHz for ^{13}C), or 800 MHz (200 MHz for ^{13}C). Chemical shift values are reported in ppm (δ) referenced to internal signals of residual protons [^{1}H NMR; C_5HD_4N (7.21); ^{13}C NMR, C_5D_5N (125.8)].

Culture growth and harvesting. *K. brevisulcata* (CAWD82) was collected from the Wellington Harbour in 1998 and is held at Cawthron Institute Culture Collection of Microalgae (CICCM), Cawthron Institute, Nelson. Bulk cultures (150-250 L batches) were grown in 12 L carboys using 100% GP+Se media under a 12/12 h day/night timed cool white fluorescent lighting regime, and with 25 min aeration every 30 min. Starter culture (14-21 days old) was added to 100% GP + Se media at a ratio of 1:10 to 1:15. Cultures were maintained for up to 21 days. Aliquots of culture were assessed for cells numbers by inverted microscopy. For ^{13}C-enrichment, cultures were augmented at 0 and 10 days with $NaH^{13}CO_3$ (0.25g per 12 L). Production of toxins was assessed by liquid chromatography – mass spectrometry (LC-MS) following SPE using a 50 mL aliquot of culture extracted with Strata-X (60 mg, Phenomenex Inc., CA), washed with Milli Q water and 20% MeOH, and eluted with MeOH or MeOH followed by acetone (3 mL each). Toxins were extracted from mature cultures using Diaion HP20 resin. Briefly, the pre-washed resin was packed in a polypropylene column. *K. brevisulcata* cultures were transferred to a 200 L barrel and cells were lysed by addition of acetone to 7% v/v. The cultures were settled for 1 h and then diluted with reversed osmosis purified water (RO water) to 5% v/v acetone before pumping at 0.3 L/min through a filter system followed by HP20 resin column. The column was then washed with water and the HP20 resin was transferred to a 2 L flask. Toxins were recovered by soaking the resin with AR acetone (1L) and decanting (x3). The combined acetone extract was rotary evaporated to produce a dried crude extract.

Isolation of KBTs. The crude HP20 extract was dissolved in MeOH and diluted to 55% v/v with pH 7.2 phosphate buffer. The solution was partitioned with $CHCl_3$ (x2) and the combined $CHCl_3$ fraction containing neutral toxins was evaporated. Brevisulcenals were isolated from the neutral fractions of 1450 L of bulk cultures by column chromatography using a diol cartridge with stepwise elution (EtOAc to MeOH) and guided by P388 cytotoxicity assay. Final purification was conducted by two stages of preparative HPLC (250 mm x 4.6 mm id Develosil C30-UG-5, Nomura Chemical Co., Japan) with isocratic elution (90% MeOH/H_2O followed by 85% MeOH/H_2O) and guided by UV absorbance at 230 nm.

Preparation of the benzene sulfonate derivative of KBT-G. KBT-G (20 μg) was treated with an excess of 3-(hydrazinecarbonyl)benzene sulfonate sodium salt for 2 h in 80% pyridine. After solvent elimination, the reaction mixture was partitioned between $CHCl_3$ and H_2O. The chloroform fraction was used for the MS/MS experiments (MALDI-SpiralTOF-TOF). The product ion spectra were analyzed using mMass software.

MALDI MS and MALDI tandem MS measurements. MALDI mass spectra were recorded on a JEOL JMS-S3000 SpiralTOF instrument using 2,5-dihydroxybenzoic acid (DHB, Wako) or α-cyano-*p*-hydroxycinnamic acid (CHCA, Wako) as matrices. The KBT-G derivative was dissolved in MeOH/$CHCl_3$ and mixed with norharmane matrix and subjected to MALDI tandem MS measurements in a negative ion mode. The product ion mass spectra were recorded with laser irradiation at 349 nm and a frequency of 250 Hz, and –20 kV of acceleration voltage in the first TOF stage. The collision energy was set at 20 keV to afford HE-CID. Product ions formed by collision-induced dissociation were re-accelerated by 9 kV for the analysis in the second TOFMS stage.

Brevisulcenal-G (2): Isolated as a colorless amorphous solid: $[\alpha]_D^{19}$ +171.2 (*c* 0.02, MeOH); UV maxima (λ) 223 (ε 12000) nm. High resolution MALDI-TOF mass spectrum of **2** gave $[M+Na]^+$ at *m/z* 2106.0584 for $C_{108}H_{162}O_{39}Na$ ($[M+Na]^+$, calcd. 2106.0585). ^1H and ^{13}C NMR data are given in Table 1.

Brevisulcenal-H (3): Isolated as a colorless amorphous solid: $[\alpha]_D^{19}$ +3.5 (*c* 0.04, MeOH); UV maxima (λ) 213 (ε 12000) nm. High resolution MALDI-TOF mass spectrum of **3** gave $[M+Na]^+$ at *m/z* 2092.0422 for $C_{107}H_{160}O_{39}Na$ ($[M+Na]^+$, calcd. 2092.0429). ^1H and ^{13}C NMR data are given in Table S1.

Brevisulcenal-I (4): Isolated as a colorless amorphous solid: $[\alpha]_D^{19}$ -16.2 (*c* 0.006, MeOH); UV maxima (λ) 212 (ε 15000) nm. High resolution MALDI-TOF mass spectrum of **4** gave $[M+Na]^+$ at *m/z* 2122.0532 for $C_{108}H_{162}O_{40}Na$ ($[M+Na]^+$, calcd. 2122.0535). ^1H and ^{13}C NMR data are given in Table S2.

ACKNOWLEDGEMENTS

We are grateful to Prof. M. Murata, Osaka University for his general gift of 3-(hydrazinecarbonyl)-benzene sulfonate sodium salt. The measurement with 800 MHz NMR spectrometer was performed under the non-proprietary use program supported by RIKEN. This work was financially supported by KAKENHI (15K01798) and a bilateral Japan-New Zealand programs funded by the Japan Society for the Promotion of Science (JSPS) and the New Zealand Ministry for Business,

Innovation and Employment (contracts CAWX0703, CAWX0804 and CAWX1108).

REFERENCES

1. F. H. Chang, *Phycologia*, 1999, **38**, 377.
2. F. H. Chang, S. M. Chistwell, and M. J. Uddstorm, *Phycologia*, 2001, **40**, 215.
3. P. T. Holland, F. Shi, M. Satake, Y. Hamamoto, E. Ito, V. Beuzenberg, P. McNabb, R. Munday, L. Briggs, P. Truman, R. Gooneratne, P. Edwards, and S. Pascal, *Harmful Algae*, 2012, **13**, 47.
4. R. Suzuki, R. Irie, Y. Harntaweesup, K. Tachibana, P. T. Holland, D. T. Harwood, F. Shi, V. Beuzenberg, Y. Itoh, S. Pascal, J. B. P. Edwards, and M. Satake, *Org. Lett.*, 2014, **16**, 5850.
5. R. Irie, R. Suzuki, K. Tachibana, P. T. Holland, D. T. Harwood, F. Shi, P. McNabb, V. Beuzenberg, F. Hayashi, H. Zhang, and M. Satake, *Heterocycles*, 2016, **92**, 45.
6. Y. Hamamoto, K. Tachibana, P. T. Holland, F. Shi, V. Beuzenberg, Y. Itoh, and M. Satake, *J. Am. Chem. Soc.*, 2012, **134**, 4963.
7. M. Satake, M. Shoji, Y. Oshima, H. Naoki, T. Fujita, and T. Yasumoto, *Tetrahedron Lett.*, 2002, **43**, 5829; M. Satake, Y. Tanaka, Y. Ishikura, Y. Oshima, H. Naoki, and T. Yasumoto, *Tetrahedron Lett.*, 2005, **46**, 3537; Y. Tanaka, M. Satake, M. Yotsu-Yamashita, and Y. Oshima, *Heterocycles*, 2013, **87**, 2037.
8. T. Satoh, T. Sato, and J. Tamura, . *J. Am. Soc. Mass Spectrom.*, 2007, **18**, 1318.
9. T. Satoh, T. Sato, A. Kubo, and J. Tamura, *J. Am. Soc. Mass Spectrom.*, 2011, **22**, 797.
10. N. Osato, H. Onoue, Y. Toma, K. Torikai, M. Ebine, M. Satake, and T. Oishi, *Chem. Lett.*, 2018, **47**, 265.
11. A. Morohashi, M. Satake, K, Murata, H. Naoki, H. F. Kaspar, and T. Yasumoto, *Tetrahedron Lett.*, 1995, **36**, 8995.
12. M. Murata, H. Naoki, S. Matsunaga, M. Satake, and T. Yasumoto, *J. Am. Chem. Soc.*, 1994, **116**, 7098.